Assessment and control of transition to turbulence

The Predictability Group Meeting, University of Oxford, Oxford, UK
October 19, 2020

Anton Pershin[1,2], Cédric Beaume[2], Steven Tobias[2]

[1]Atmospheric, Oceanic and Planetary Physics, University of Oxford
[2]School of Mathematics, University of Leeds

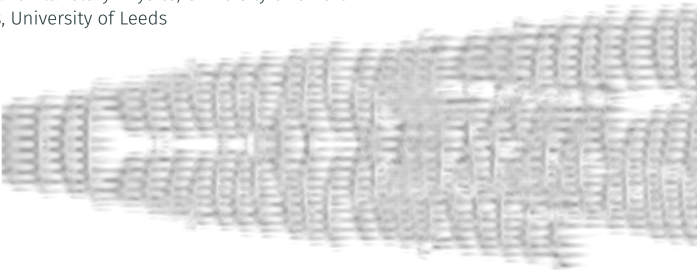

Reynolds experiment

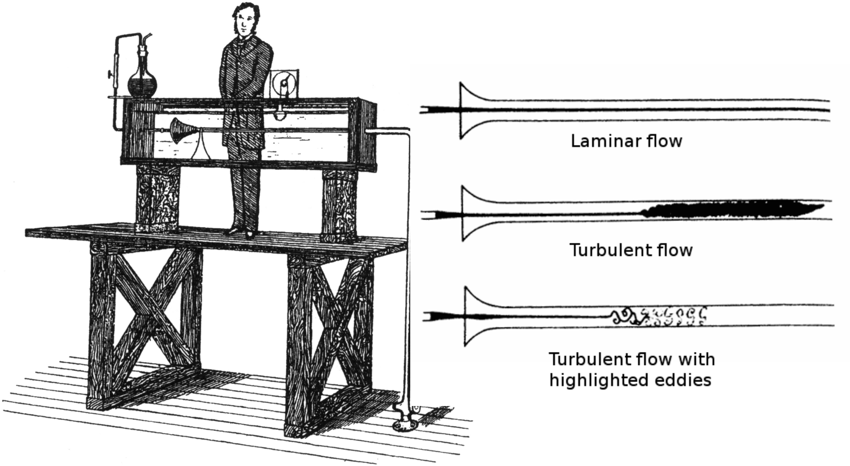

Reynolds, Phil. Trans. R. Soc. London, 174 (1884)

Plane Couette flow

Navier–Stokes equation:

$$\partial_t \boldsymbol{u} + (\boldsymbol{u} \cdot \nabla)\boldsymbol{u} = -\nabla p + \frac{1}{Re}\nabla^2 \boldsymbol{u}$$

Incompressibility condition: $\nabla \cdot \boldsymbol{u} = 0$

Streamwise and spanwise directions: periodic BCs

Wall-normal direction: no-slip BCs

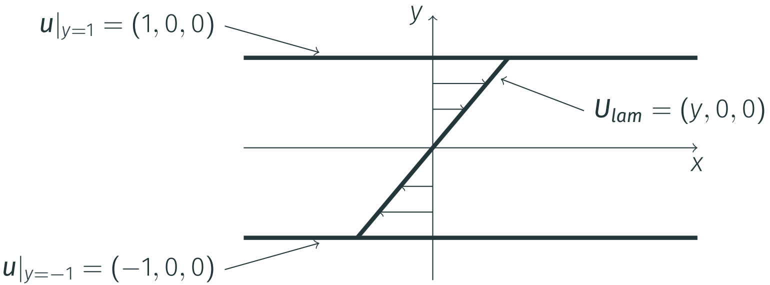

Subcritical transitional flows

	Linearly stable laminar state	Sustained turbulence
Plane Couette flow	all *Re*	$Re \gtrsim 325$
Pipe flow	all *Re*	$Re \gtrsim 2040$
Plane Poiseuille flow	$Re \lesssim 5772$	$Re \gtrsim 840$

Transition is complicated by the coexistence of two attractive states:

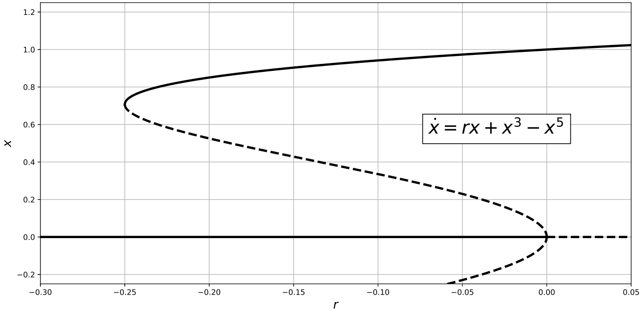

Edge of chaos is wrapped up around the turbulent saddle[1]

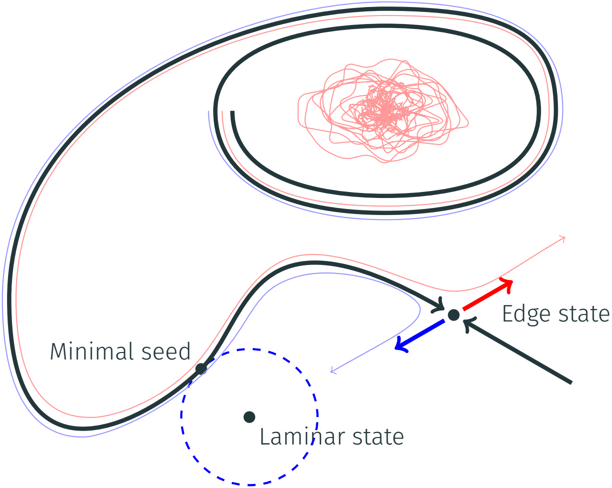

[1] Chantry *et al.*, J. Fluid Mech. **747** (2014)

Edge tracking

Edge tracking allows to compute edge states

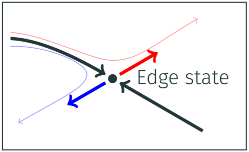

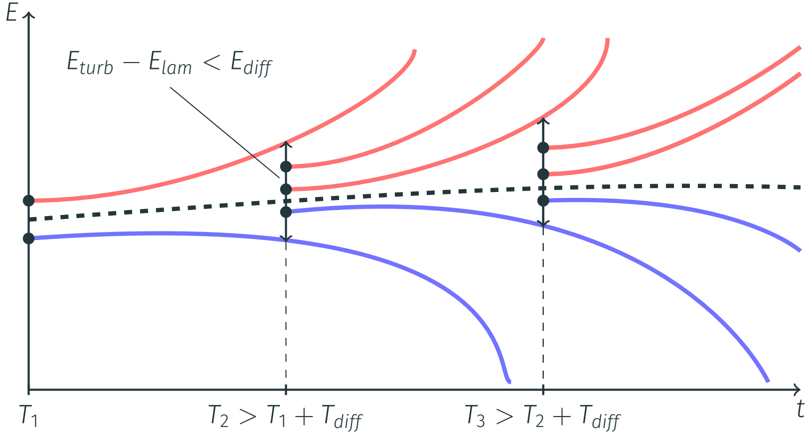

Transition and control in a small domain

Edge states in plane Couette flow

Edge states are equilibria in small domains:[2]

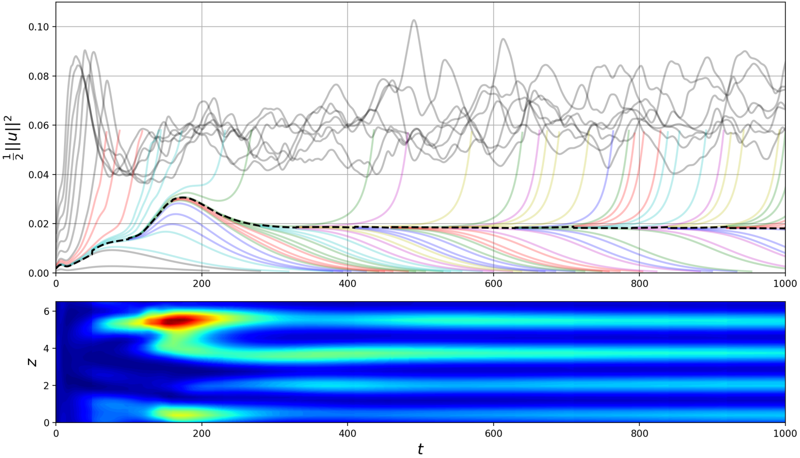

Top plot: initial trajectories (gray), following iterations (color) and edge trajectory (dashed).
Bottom plot: edge trajectory represented via *xy*-averaged kinetic energy.

[2] Schneider *et al.*, Phys. Rev. E, 76, 016301 (2007)

How robust is the laminar state to perturbations?

Indicators of stability:

- Infinitesimal perturbations $\Longrightarrow$ linear growth rate
- Finite-amplitude perturbations $\Longrightarrow$ the size of the basin of attraction

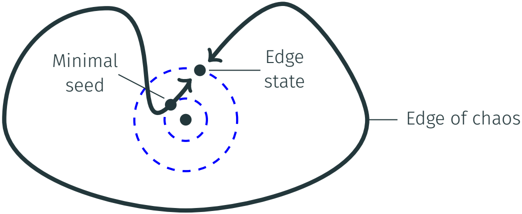

Laminarisation probability $P_{lam}(E)$ is the probability
that a random finite perturbation of energy E laminarises

Random perturbation:

$$\boldsymbol{u} = A\boldsymbol{u}_\perp + B\boldsymbol{U}_{lam},$$

where $A, B, \boldsymbol{u}_\perp$ are generated randomly and $\langle \boldsymbol{u}_\perp, \boldsymbol{U}_{lam} \rangle = 0$

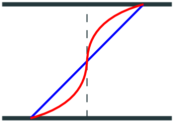

Laminarisation probability

- $P_{lam}(E)$ approximates the size of the basin of attraction
- Laminarisation probability fitting: $p(E) = 1 - (1 - a)\gamma(\alpha, \beta E)$
- Control strategies can be assessed by comparing $P_{lam}(E)$

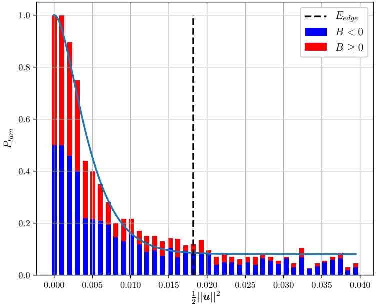

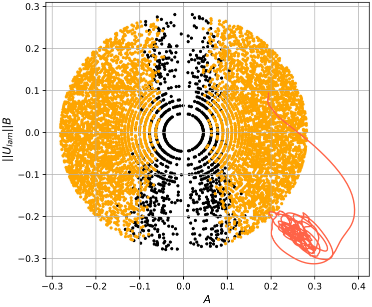

Left: laminarisation probability for perturbations with energies between 0 and $2E_{edge}$
Right: random perturbations classified as laminarising (black) and transitioning (yellow)

Control strategy: wall oscillations

We impose in-phase oscillations on the walls[3]:

$$\boldsymbol{u}(x, \pm 1, z, t) = \pm \boldsymbol{e_x} + A sin(\omega t) \boldsymbol{e_z}$$

$$\implies \quad \boldsymbol{U_{lam}} = y \boldsymbol{e_x} + W(y, t) \boldsymbol{e_z}.$$

(a) $t = 0$: (b) $t = \frac{\pi}{2\omega}$: (c) $t = \frac{\pi}{\omega}$: (d) $t = \frac{3\pi}{2\omega}$:

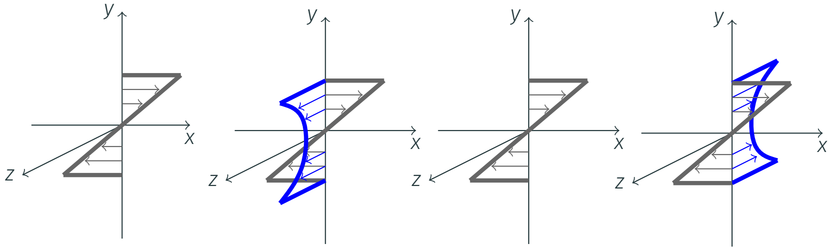

[3] Motivated by Rabin *et al.*, J. Fluid Mech. 738 (2014)

Edge state for wall-oscillated flow

- Consider $A = 0.3$ and $\omega = 1/16 \implies$ the edge state is chaotic
- The average E_{edge} is decreased by approximately 37%

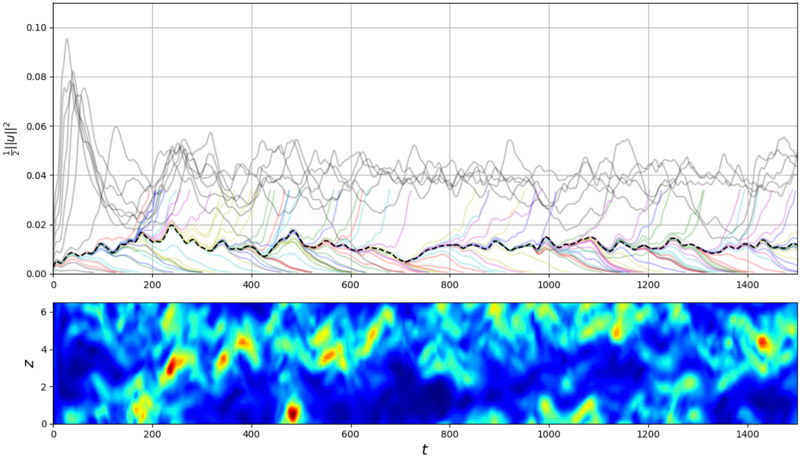

Top plot: initial trajectories (gray), following iterations (color) and edge trajectory (dashed).
Bottom plot: edge trajectory represented via xy-averaged kinetic energy.

Laminarisation probability for wall-oscillated flow

- P_{lam} is significantly increased compared to the uncontrolled case
- Relative probability increase:

$$\frac{1}{2E_{edge}} \int_0^{2E_{edge}} \frac{p_{osc}(E) - p(E)}{p(E)} dE \approx 1.8$$

- Laminarising perturbations are spread all over the space $(A, ||\boldsymbol{U}_{lam}||B)$

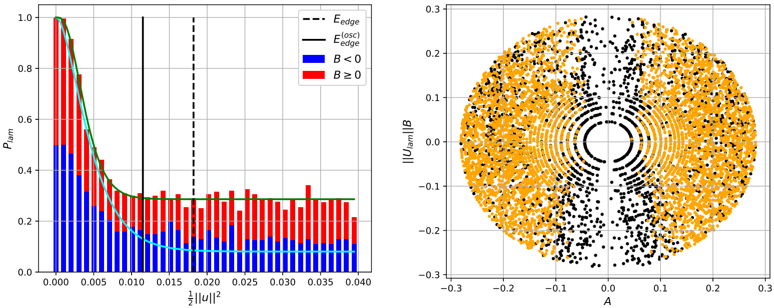

Left: laminarisation probability for perturbations with energies between 0 and $2E_{edge}$
Right: random perturbations classified as laminarising (black) and transitioning (yellow)

Optimal control with respect to laminarisation probability

- Wish to find A and ω maximising the laminarisation probability
- Use only a small number of random perturbations
- Employ Bayesian estimation to quantify the uncertainty

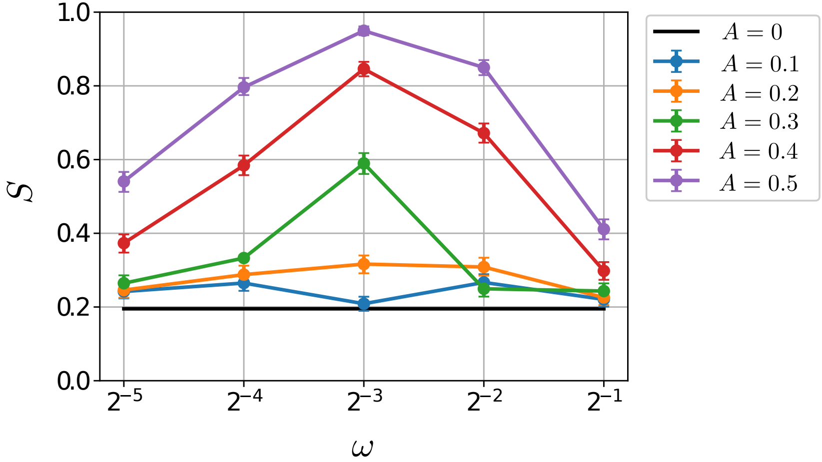

Transition to turbulence in a wide domain

Localised edge states

(a) $63.7\pi \times 2 \times 15.9\pi$ domain[4]:

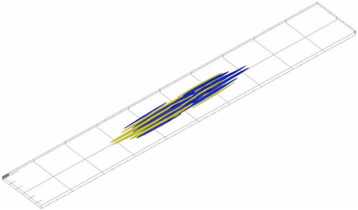

(b) $64\pi \times 2 \times 16\pi$ domain[5]:

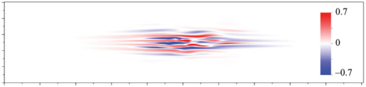

(c) $4\pi \times 2 \times 8\pi$ domain[5]:

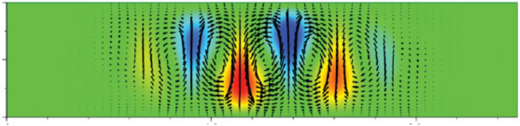

[4] Duguet *et al.*, Phys. Fluids, 21, 111701 (2009)
[5] Schneider, *et al.*, J. Fluid Mech., 646 (2010)

Snaking in plane Couette flow ($4\pi \times 2 \times 32\pi$)

- First observed by Schneider *et al.* in 2010[6]
- Homoclinic snaking is most studied for the Swift–Hohenberg equation[7]

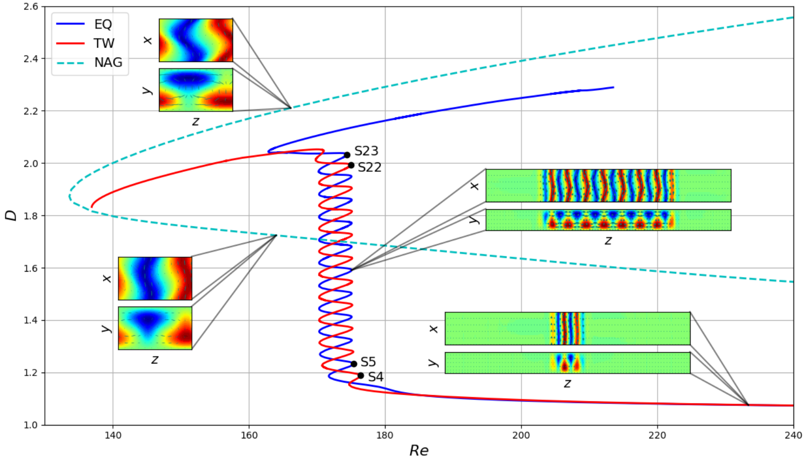

[6]Schneider *et al.*, Phys. Rev. Lett., **104** (2010)
[7]Knobloch, Annu. Rev. Condens. Matter Phys., **6** (2015)

Depinning

- **Depinning** is the process of expansion/collapse of the initial spatial pattern outside the snaking by nucleation/annihilation of cells
- Square-root law of the speed of fronts: $c \propto |Re - Re_s|^{1/2}$
- Depinning in plane Couette flow was witnessed by Duguet *et al.*[8]

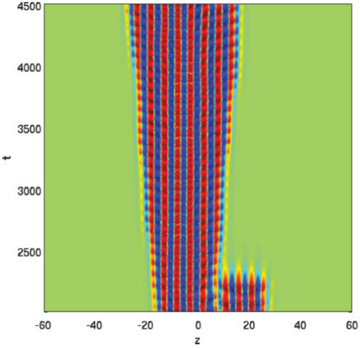

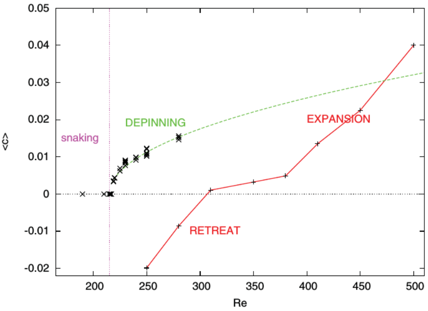

[8] Duguet *et al.*, Phys. Rev. E, 84 (2011)

Relaminarisation times for localised states

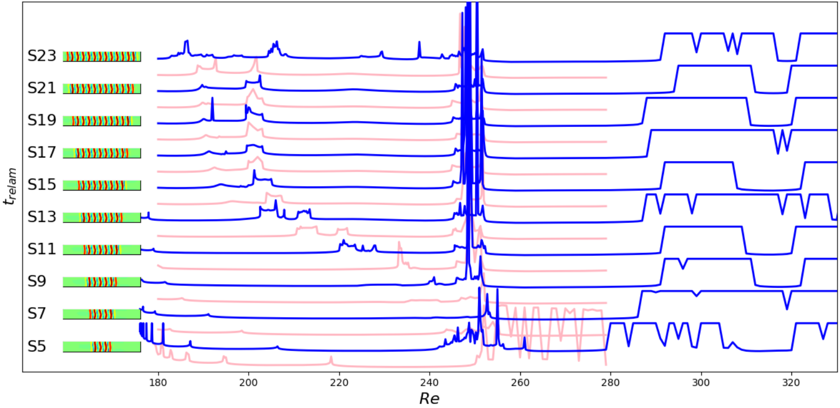

Relaminarisation times for EQ (blue) and TW (red) saddle-node states. Midplane of streamwise velocity of EQ saddle-node states is shown on the left.

No major difference between the dynamics of EQ and TW

Relaminarisation times for localised states

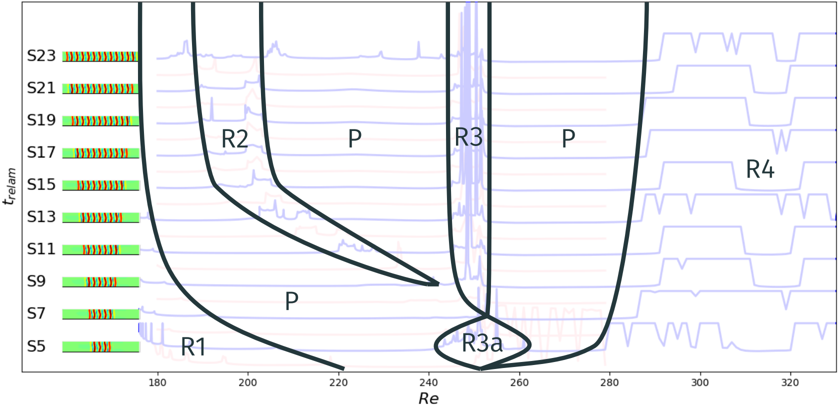

Relaminarisation times for EQ (blue) and TW (red) saddle-node states. Midplane of streamwise velocity of EQ saddle-node states is shown on the left.

No major difference between the dynamics of EQ and TW

Region R1 – peaks (S5)

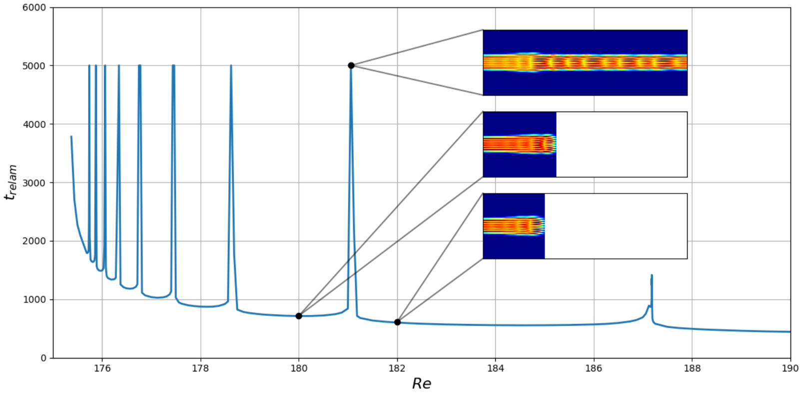

- Peaks: $Re_{n+1} - Re_s = \alpha\,(Re_n - Re_s)$
- Local minima: $t_n = t_0 + \beta n$

$$\Longrightarrow \quad t_{relam} = \frac{\beta}{\ln\alpha} \ln\left[\frac{2\,(Re - Re_s)}{(1+\alpha)\,(Re_0 - Re_s)}\right] + t_0$$

Region R2 – splitting

- Region R2 appears due to the creation and activation of spots
- The spot size is the same for all considered initial conditions

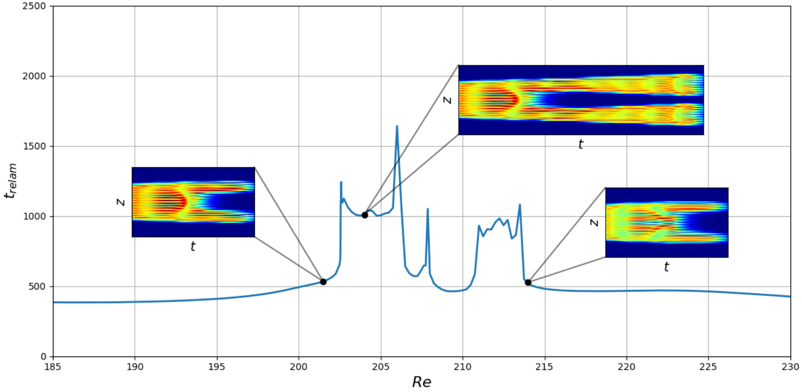

Relaminarisation times for S13 integrated for $Re \in [185; 230]$.

Region R3 – chaotic transients

- Like R2, R3 originates from the splitting of the initial spot
- Unlike R2, R3 contains long-lasting chaotic transients ($T > 4000$)
    - Decay of roll clusters overwhelms front propagation

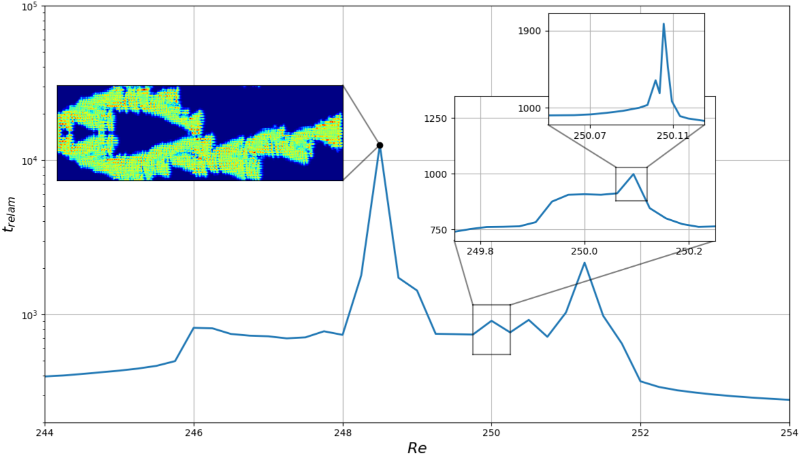

Relaminarisation times for S9 integrated for $Re \in [244; 254]$.

Region R4 – transition to turbulence

- Front propagation overwhelms decay of roll clusters
- Average front speed $\langle c \rangle = 0.02$ does not depend on Re for $Re < 350$

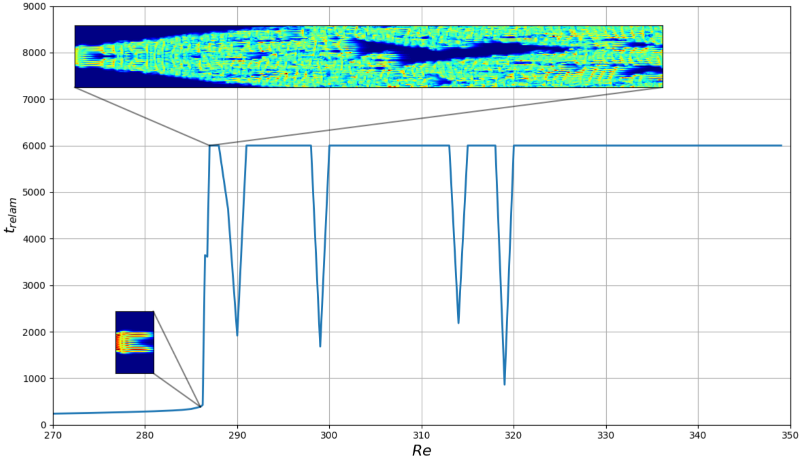

Relaminarisation times for S7 integrated for $Re \in [270; 350)$ and cut at $t_{relam} = 6000$.

Control of transition in a wide domain

Homotopy from the uncontrolled system for S5

- Control strategies can be assessed by comparing t_{relam}
- Consider in-phase wall oscillations with $\omega = 1/16$
  - Fast relaminarization for $A \sim O(10^{-1})$
  - Original regions are recovered for $A \lesssim 10^{-2}$

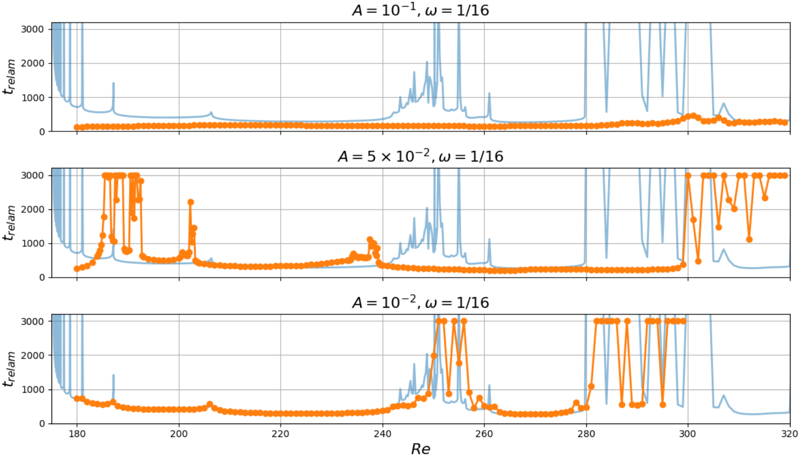

Homotopy from the uncontrolled system for S13

- Fast relaminarization for $A \sim O(10^{-1})$
- Original regions are recovered for $A \lesssim 10^{-3}$

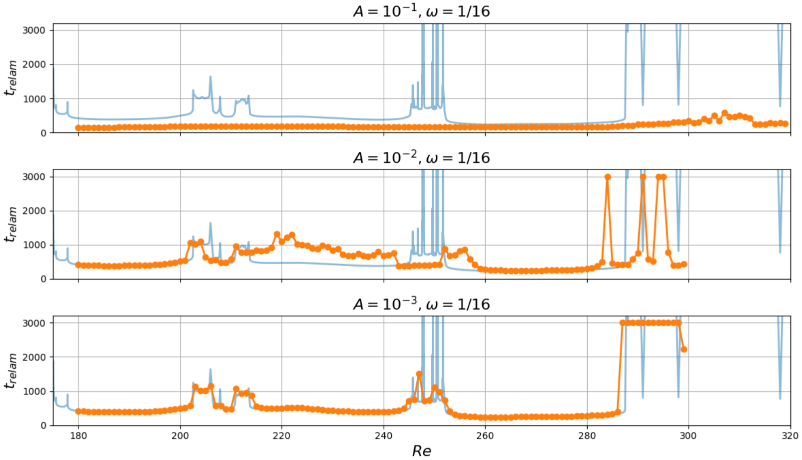

Relaminarisation times for the uncontrolled (blue) and wall-oscillated (orange) cases.

The onset of transition to turbulence

- For amplitudes $A \gtrsim 10^{-1}$, the only existing region is R4
- Increasing A delays the onset of R4
- Frequency $\omega = 1/8$ is the most efficient in delaying the onset

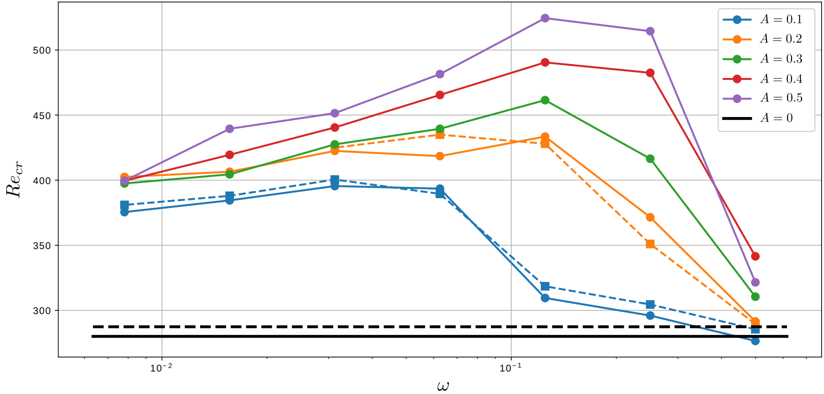

Critical Reynolds number as a function of the amplitude A and the frequency ω of the wall oscillation. Solid lines correspond to S5 and dashed lines correspond to S13.

Stages of transition

Wall oscillations favour directed-percolation-like transition [9,10]:

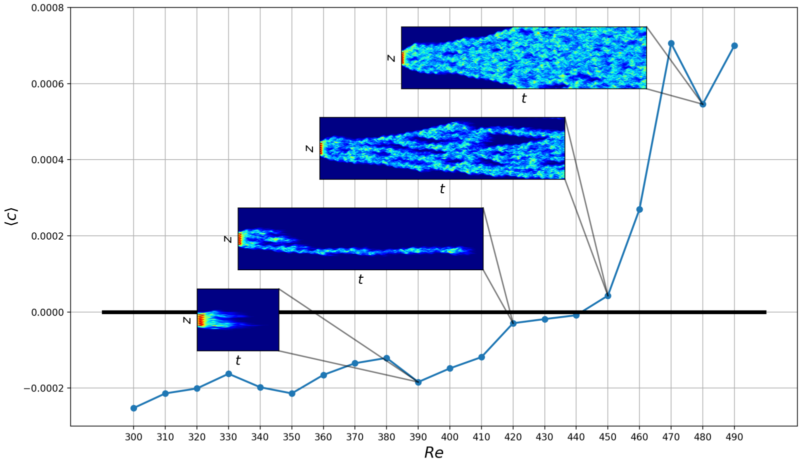

[9] Sipos and Goldenfeld, *Phys. Rev. E* 84, 035304 (2011)
[10] Chantry *et al.*, *J. Fluid Mech.* 824, R1 (2017)

Conclusion

Laminarisation probability:

- Helps analyse finite-amplitude instabilities
- Approximates the size of the basin of attraction
- Allows to quantify and compare the efficiency of control strategies
- Minimal seeds and edge states may be misleading while designing control

Pershin, Beaume and Tobias, *J. Fluid Mech.* 895, A16 (2020)

Transition in a wide domain:

- Exact solutions are reproducible initial conditions
- Characterise transitional dynamics via relaminarisation times
- Exact solutions + relaminarisation times = framework
  $\Longrightarrow$ Assessment of control strategies

Pershin, Beaume and Tobias, *J. Fluid Mech.* 867, 414–437 (2019)